Chinese Chemical Letters 31 (2020) 2091–2094

Contents lists available at ScienceDirect

Chinese Chemical Letters

journal homepage: www.elsevier.com/locate/cclet

Communication

Morphology evolution of ZnO by controlling solvent and electrochemical sensing of hexagonal nanotablets toward amines

Md. Maruf Ahmed[a], Ruihua Zhao[a,b,*], Bayram Hayytov[a], Yangyang Shang[a], Jinping Li[a,c,*], Jianping Du[a,c,*]

[a] College of Chemistry and Chemical Engineering, Taiyuan University of Technology, Taiyuan 030024, China
[b] Shanxi Kunming Tobacco Co., Ltd., Taiyuan 030032, China
[c] Shanxi Key Laboratory of Gas Energy Efficient and Clean Utilization, Taiyuan 030024, China

ARTICLE INFO

Article history:
Received 11 December 2019
Received in revised form 29 December 2019
Accepted 30 December 2019
Available online 9 January 2020

Keywords:
ZnO
Morphology control
Hexagonal nanotablet
Electrochemical sensor
Organoamines

ABSTRACT

Organic amines are important solvent and raw material in laboratory and industry, as well as releasing from cigarette smoke. It is significant to detect low-concentration amines for environment and public health. Here we reported that as-synthesized zinc oxide is an effective electrode material of electrochemical sensor for the detection of amines. The characterization results reveal that the ZnO morphologies experienced a change from hexagonal bowl-like microparticles, cones, prisms to nanoparticles by adjusting the reaction time, temperature, solvents and additives. Interestingly, ZnO material possessing hexagonal shapes and different sizes exhibits distinct electrochemical response in various amines solution, suggesting that there is a better dependent relationship between different morphological ZnO and amines detection. Particularly, regular hexagonal ZnO nanotablets exhibit a detectable electrochemical response and selectivity to ammonia, implying it can be serve as electrode material for highly effective detection of organic amines.

Environmental pollution from organic substances leads to great harm to people's health and life. Organic amine is important solvent, raw material and it is also one of components in cigarette mainstream and sidestream smoke [1]. Thus, it is more important and necessary to detect amines because volatile organoamines are one of very poisonous and harmful VOCs and can cause more menace to human life, health and environment [2]. The common methods for detection of organoamines include optical sensing [3] and fluorescent probes [4]. Most of these detection methods are costly or complicated to be employed, whereas chemical sensors are simple and convenient to be used to detect volatile organic amines (VOAs) including dimethylamine [5], trimethylamine [6], triethylamine [7,8].

Presently, semiconductor nanomaterials (WO_3, SnO_2, ZnO, *etc.*) and its devices for detection of volatile and toxic compounds are of interest in the sensor areas [9–14]. Among of semiconductor oxides, zinc oxide is one of the most important n-type semiconductor materials, and it possesses a wide direct band gap (3.37 eV) and a strong excition binding energy (60 MeV) at room temperature [14]. Therefore, zinc oxide is a versatile material and it is promising for different applications such as solar cells [15], field-effect transistors [16], photocatalysts [17] and chemical sensors [18,19]. In particular, it is commonly used to detect a range of flammable, toxic and harmful gases as well as volatile organic compounds (VOCs), including H_2 [20], formaldehyde [21], ethanol [22], acetone [23] and aromatic compounds [24].

As we know, gas-sensing property of zinc oxides is dependent on their morphologies. For example, the pencillike ZnO, prism and microflowers structural ZnO exhibits different responses in detection of triethylamine [7,8]. To date, the more efforts have still been made to develop ZnO materials with controlled structure and morphology for improvement of sensing performance such as gridlike lamellae [14], flowerlike [25], nanowires [26] and mesopore [27]. Recently, our work focused on morphology engineering of 2D/3D ZnO for improvement of its sensing properties in triethylamine detection and the results show that there is an obvious effect of morphology on gas response [28]. From aforementioned, more reported works are the detection of

* Corresponding authors at: College of Chemistry and Chemical Engineering, Taiyuan University of Technology, Taiyuan 030024, China.
E-mail addresses: zhrh6688@163.com (R. Zhao), jpli211@hotmail.com (J. Li), dujp518@163.com (J. Du).

https://doi.org/10.1016/j.cclet.2020.01.014
1001-8417/

gaseous amine. However, the detection of liquid amines or amine solutions also cannot be ignored. Ameen *et al.* reported an electrochemical method to detect liquid ethanolamine effectively using ZnO nanotubes as electrode [29]. Du *et al.* synthesized star-shaped ZnO microparticles self-assembled from hexagonal prisms and used for electrochemical detection of ethylenediamine [30]. Yang *et al.* investigated that a novel single-walled carbon nanotubes array-modified glassy carbon electrode showing the excellent electrocatalytic performance of as-fabricated electrode toward dopamine [31]. Comparatively, the detection of organic amines in solution is still few reported.

Herein, series of ZnO micro-/nanoparticles with tailored morphologies were synthesized by using the solov/hydrothermal method and the electrochemical sensing properties were studied in amine solution.

The morphology, structure and size of ZnO strongly depend on reaction time, reaction temperature, solvents and CTAB. Morphology evolutions of ZnO micro-/nanoparticles were studied by exploring the influenced factors. The growth routes are shown in Scheme 1.

Fig. 1 indicates the effect of reaction time on size and morphology of ZnO. Clearly, as-synthesized ZnO material is comprised of well-dispersed microparticles and the sizes are about less than 5 μm (Fig. 1a). Several microparticles were magnified and displayed in Figs. 1b and c. From top-view images, ZnO microparticles have hexagonal contours and side-view shows a very similar bowl-like shape, with the thick of more than 1 μm, and the size of about 3 and 3.8 μm, which was formed by adhesion of large particle and small hexagonal tablet. After a long reaction time, ZnO microparticles keep hexagonal shapes and the bowl-like particles are not observed (Fig. 1d). Perfect hexagonal particles with clear contours were formed and their sizes are about 2.5 and 4 μm (Figs. 1e and f). The results indicate that the ZnO microparticles experience growth evolution from bowl-like to perfect hexagonal brick-like shape driven by enough reaction time. All XRD peaks of the HZOM-6 and HZOM-10 material at 31.75, 34.43, 36.28, 47.54, 56.70, 62.84, 67.92 and 69.08 degrees can be assigned to the reflections of the (100), (002), (101), (102), (110), (103), (112) and (201) planes of ZnO, respectively (Fig. S1 in Supporting information), which can be indexed as the hexagonal ZnO wurtzite structure (JCPDS card No. 36-1451). No impurity peaks are observed in the XRD pattern, implying as-synthesized materials can be said to be exclusively composed of ZnO.

The reaction temperatures affect the growth of ZnO microparticles (Fig. S2 in Supporting information). Several large particles with hexagonal morphology and small irregular blocks are observed (Fig. S2a). A single particle with the size of *ca.* 6.5 μm magnified (Fig. S2b) possesses clear hexagonal contour and consists of irregular blocks. As the temperature rose, the ZnO microparticles trend to grow into larger particles with indistinct hexagonal contour and a uniform size of 8 μm (Fig. S2c). The

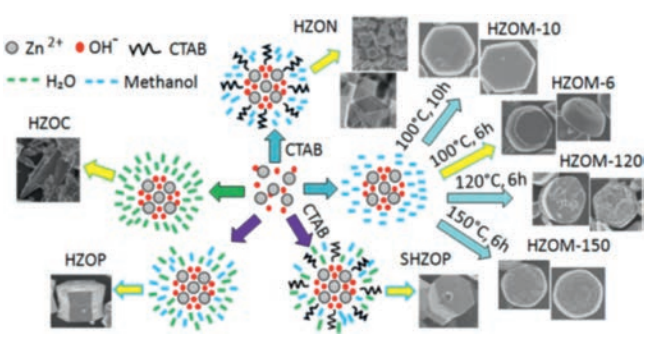

Scheme 1. Growth routes of ZnO micro/nanopartcles with different hexagonal structure.

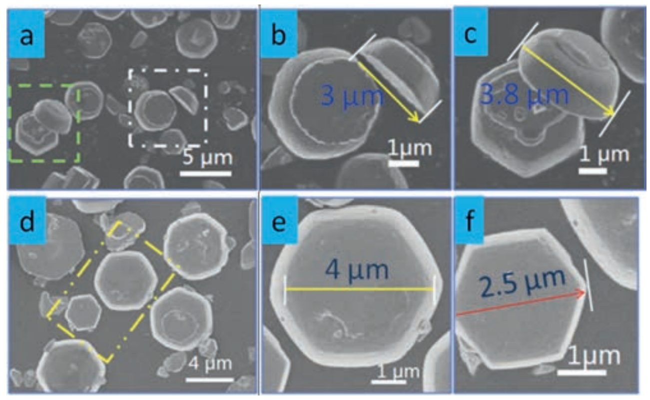

Fig. 1. SEM images of ZnO microparticles in the present of methanol as solvent. (a–c) HZOM-6, (d–f) HZOM-10.

magnified image shows large microparticles formed by small particles fusing together completely (Fig. S2d), suggesting high reaction temperature favor the growth of better crystal with smooth surface. The XRD patterns show that ZnO prepared at high temperature has high crystalline and hexagonal wurtzite structure (Fig. S3 in Supporting information).

To have an insight into the effect of solvents, ZnO was synthesized by using water and methanol/water as solvents, respectively. In water system, as-synthesized ZnO composes of microparticle with hexagonal-cone shape (Fig. S4a in Supporting information). Whereas, in methanol/water mixed solvent, short hexagonal prisms consisting of two overlapped hexagonal brick-like particles were observed and their size are about 10 μm (Fig. S4b in Supporting information). Morphology difference may be ascribed to polarity of solvents. Weak polar solvent make ZnO particles longitudinal growth dominate and strong polar solvent favour ZnO growth along horizontal and longitudinal directions. Similar morphological ZnO microparticles with the size of 5 μm, which was obtained by adding CTAB in mixed solvent, was observed in Fig. S4c (Supporting information). The size is less than one prepared without CTAB and these particles are more uniform and their surface are smooth, resulting from effect of CTAB's dispersion-inhibited growth of ZnO. All the characteristic peaks (Fig. S4d in Supporting information) are indexed in line with the wurtzite structure (JCPDS No. 36-1451).

Hexagonal ZnO nanoparticles (HZON) were synthesized by adding CTAB in methanol solvent. SEM image show ZnO material composed of uniform and well-dispersed nanoparticle with hexagonal tabletlike shape (Fig. 2a). The reason is that CTAB can form reverse micelles in methanol system and restrain ZnO growth effectively. As-synthesized ZnO nanoparticles have a hexagonal wurtzite structure (Fig. 2b), which was confirmed by the characteristic peaks of ZnO (JCPDS No. 36-1451). EDS analysis show several peaks corresponding to only zinc and oxygen, besides one that is due to copper from the copper grid (Fig. 2c), which provided another evidence that hexagonal tablet-shaped microparticles are exclusively composed of ZnO. The size distribution of selected area (Fig. 2a) is shown in Fig. 2d. Obviously, the sizes of microparticles are in the range of 170–230 nm and the most is about 200 nm, indicating very good uniformity.

TEM images of HZON also show the presence of particles with a hexagonal tablet-like morphology (Fig. 2e), just like those seen in the SEM images above. ZnO particles are very regular hexagonal two-dimension nanosheets and they have uniform size of *ca.* 200 nm. The typical nanoparticles are displayed in Fig. 2f and their fine structures are further observed. The lattice fringes, indicating the highly crystalline nature of the hexagonal nanosheet, can be clearly seen (Figs. 2g and h). The average interlayer

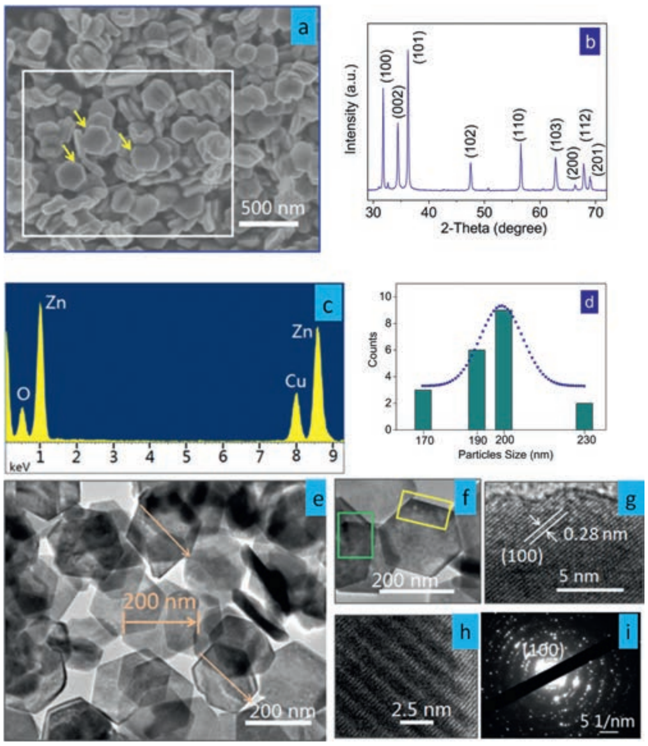

Fig. 2. (a) SEM image and (b) XRD pattern of ZnO nanoparticles prepared in present of CTAB and methanol as solvent (HZON). (c) EDS spectrum and (d) size distributions of selected area in Fig. 2a. (e, f) TEM and (g, h) HRTEM images and the selected area electron diffraction pattern (e) of HZON sample.

distance is found to be about 0.28 nm (Fig. 2g), which corresponds to the characteristic d-spacing value of the (100) facet of ZnO, further suggesting that the hexagonal ZnO nanosheet have the wurtzite structure. The selected area electron diffraction (SAED) pattern show characteristic of polycrystalline ZnO and small ring corresponds to ZnO diffraction of (100) plane, indicating a hexagonal wurtzite structure (Fig. 2i).

HZOM-10-based electrode exhibits a strong response to DMA than the HZOM-6′s (Fig. S5a in Supporting information). It is found that HZOM-6-based electrode exhibits a high response to NH_4OH among other amines, but only slight higher than the response of HZOM-10′s material. The reasons may be ascribed to the size and surface defect of bowl-like and hexagonal ZnO microparticles and the former may provide much active sites. A linear scan voltammetry result shows the current arises when DMA is present in PBS and its value increases as a function of the DMA concentration (Fig. S5b in Supporting information). This clearly indicates that the HZOM-10-coated GCE responds to DMA, in a concentration-dependent manner. The relatively high current suggests that hexagonal ZnO microparticles can serve as an effective electrochemical sensor for the detection of DMA. It is interesting that there is good linearity (R^2 = 96%) between concentration and response to DMA in the range of 40–200 ppm (Fig. S5c in Supporting information). These results indicate that HZOM-10 may serve as a sensitive material for DMA detection and it is also a powerful tool to quatitative analyze DMA in our environment.

Similarly, electrochemical sensing properties of hexagonal ZnO microparticles with different sizes were investigated. HZOM-120 based electrode exhibits an obvious response to TMA than the other organ-amines (Fig. S6a in Supporting information). HZOM-120 microparticles exhibit a high selectivity to TMA compared with HZOM-100 (HZOM-6) and HZOM-150 during electrochemical detection in solution. The linear scan voltammetry result shows the current arises only when TMA is present in PBS and its value increases with increasing TMA concentration (Fig. S6b in Supporting information), which clearly indicates that the electrochemical responds to TMA in a concentration-dependent manner. Especially, it is observed that there is good linearity (R^2 = 99%) between concentration and response to TMA (Fig. S6c in Supporting information), which suggests that hexagonal microparticles self-assembled with irregular blocks can serve as an effective electrochemical sensor for the detection of TMA and also be used to quantitatively test TMA with possible concentration in our daily environment.

Compared with microparticles, hexagonal ZnO nanoparticles (HZON) is more suitable to detect weak reducing amine. As observed, the electrode exhibits a distinguishable response to NH_4OH compared to the other organ-amines (Fig. 3a). Thus, it has a detectable selectivity to NH_4OH during electrochemical detection in solution. A linear scan voltammetry result shows the current arises as a function of the NH_4OH concentration when NH_4OH is present in PBS (Fig. 3b). This behavior clearly indicates that the HZON-coated GCE responds to NH_4OH in a concentration-dependent manner. The more importance is that the good linearity (R^2 = 99%) between concentration and response to ammonia is confirmed in the large concentration range of 40–200 ppm (Fig. 3c).

The electrochemical performances were tested in different amines including ammonia (NH_4OH), diethylamine (DEA), dimethylamine (DMA), triethylamine (TEA) and trimethylamine (TMA). Clearly, the electrochemical responses are strong dependent on ZnO's morphology and size (Fig. 3d). The tablet-like nanoparticles (HZON) sample exhibits a high selectivity to NH_4OH, whereas hexagonal ZnO microparticles (HZOM-120 and HZOM-150) and hexagonal cone (HZOC) samples shows high selectivity to TMA (Fig. S7 in Supporting information), and only hexagonal microparticles (HZOM-10) with small size exhibits a notable response to DMA.

The reaction mechanism of the ZnO material as electrode is shown in Scheme S1 (Supporting information). When electrode is exposed in air, the oxygen molecules are adsorbed onto the surfaces of ZnO nanoparticles, and then capture electrons and form various adsorbed $O^{\alpha-}$ (O^{2-}, O^- and O^{2-}) ions [32]. When the ZnO-coated electrode is immersed in ammonia solution, small ammonia molecules react easily with adsorbed oxygen ions, and then adsorbed oxygen release electrons back to sensor material, which leading to redox reaction. The equation is simply described as follows,

$$NH_3OH + O^{\alpha-}\ (ads) \rightarrow H_2O + N_2 + e^-$$

In a word, hexagonal ZnO nanotablets can adsorb more oxygen molecules on their surface compared with other morphological ZnO micorparticles, which favors the reaction of weak reductive amine with oxygen ions. The results imply the electrochemical sensor is an effective tool for the detection of various amines by using different morphological ZnO as electrode material.

A series of ZnO materials were obtained by solvo/hydrothermal route. The morphology evolution from micrometer bowllike particle, cones, prism to nanotablets was achieved controllably. In the detection of amines (40−200 ppm), as-synthesized ZnO are effective electrochemical sensor material and there is a strong dependent on morphology and structure of ZnO. The different morphological ZnO can detect different amines. Notably, hexagonal ZnO nanotablet exhibits a distinct sensitivity and selectivity to ammonia and its response value is much 1.5 and 4 times than those of ZnO microparticle and prisms' ones. The results show that the amine detection will be realized by adjusting ZnO morphology and

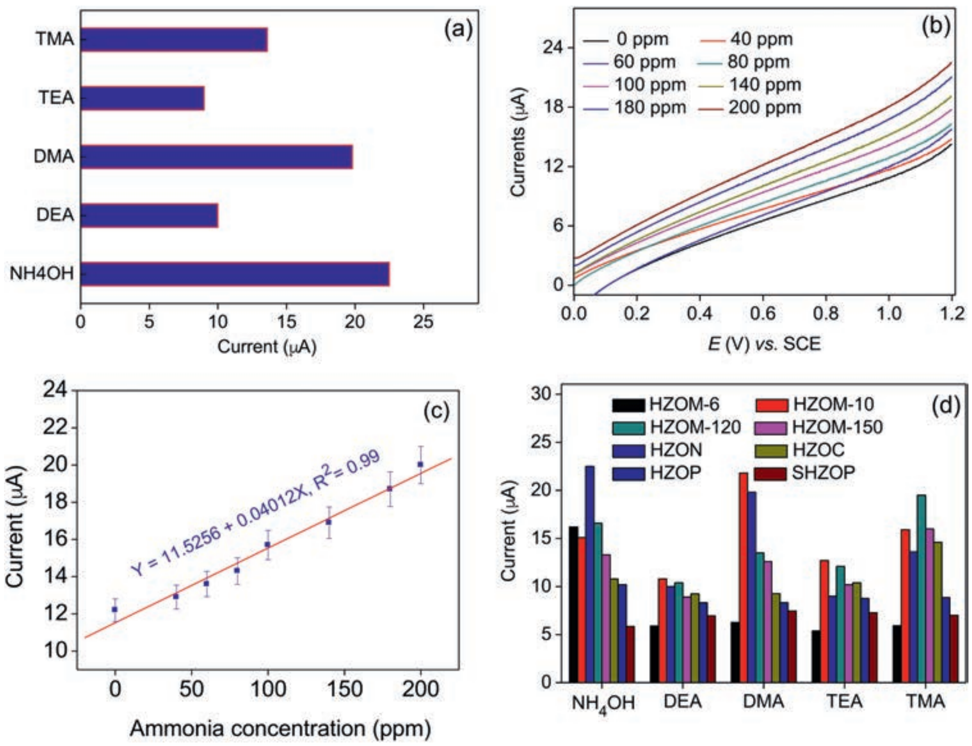

Fig. 3. (a) Current responses of HZON to different amines with 200 ppm. (b) Responses to ammonia with different concentrations. (c) Line relations of ammonia concentrations and responses to ammonia at 1.2 V. (d) Current responses to various amines with 200 ppm in PBS solution.

nano-ZnO tablets are a promising electrode material for electrochemical detection of ammonia.

Declaration of competing interests

The authors declare that they have no known competing financial interests or personal relationships that could have appeared to influence the work reported in this paper.

Acknowledgments

The authors thank National Natural Science Foundation of China (No. 51572185), Natural Science Foundation of Shanxi Province (No. 2014011016-4) and Key R&D program of Shanxi Province (International Cooperation, No. 201903D421079) for the financial support. This work was also supported by Shanxi Province Technology Foundation for Selected Overseas Chinese Scholar, Research Project Supported by Shanxi Scholarship Council of China, College Student Innovation Program of Shanxi (Nos. 2017550, 2018081) and National College Student Innovation and Entrepreneurship Training Program (No. 201910112002).

Appendix A. Supplementary data

Supplementary material related to this article can be found, in the online version, at doi:https://doi.org/10.1016/j.cclet.2020.01.014.

References

[1] Y. Inaba, S. Uchiyama, N. Kunugita, Environ. Health Prev. Med. 23 (2018) 1–7.
[2] Y. Xie, J. Du, R. Zhao, H. Wang, H. Yao, J. Environ. Chem. Eng. 1 (2013) 1380–1384.
[3] R.K. Sonker, S. Sikarwar, S.R. Sabhajeet, Rahul, B.C. Yadav, Optical Mater. 83 (2018) 342–347.
[4] Y. Fu, W. Xu, Q. He, J. Cheng, Sci. China Chem. 59 (2016) 3–15.
[5] J. Du, H. Wang, R. Zhao, Y. Xie, H. Yao, Mater. Lett. 107 (2013) 259–261.
[6] D. Meng, D. Liu, G. Wang, et al., Appl. Sur. Sci. 463 (2019) 348–356.
[7] J. Du, H. Yao, R. Zhao, et al., Mater. Lett. 136 (2014) 427–430.
[8] D. Meng, J. Si, M. Wang, et al., Chin. Chem. Lett. (2019), doi:http://dx.doi.org/10.1016/j.cclet.2019.12.021.
[9] Y. Ren, Y. Zou, Y. Liu, et al., Nat. Mater. 19 (2020) 203–211.
[10] J. Du, R. Zhao, Y. Xie, J. Li, Appl. Sur. Sci. 346 (2015) 256–262.
[11] S. Chen, Y. Qiao, J. Huang, et al., RSC Adv. 6 (2016) 25198–25202.
[12] Q. Wang, L. Bao, Z. Cao, et al., Chin. Chem. Lett. (2019), doi:http://dx.doi.org/10.1016/j.cclet.2019.12.007.
[13] L. Wang, H. Fu, Q. Jin, et al., Sens. Actuator. B -Chem. 292 (2019) 148–155.
[14] J. Du, R. Zhao, S. Chen, et al., ACS Appl. Mater. Interfaces 7 (2015) 5870–5878.
[15] J. Xu, Z.H. Chen, J.A. Zapien, C.S. Lee, W. Zhang, Adv. Mater. 26 (2014) 5337–5367.
[16] H. Frenzel, A. Lajn, H. von Wenckstern, et al., Adv. Mater. 22 (2010) 5332–5349.
[17] E. Jang, J. Won, S. Hwang, J. Choy. Adv. Mater. 18 (2006) 3309–3312.
[18] P. Ding, D. Xu, N. Dong, et al., Chin. Chem. Lett. (2019), doi:http://dx.doi.org/10.1016/j.cclet.2019.11.024.
[19] J. Du, J. Wu, R. Zhao, et al., Mater. Today Proc. 3 (2016) 345–349.
[20] R. Zhou, G. Hu, R. Yu, C. Pan, Z.L. Wang, Nano Energy 12 (2015) 588–596.
[21] N. Zhang, L. Yan, Y. Lu, et al., Chin. Chem. Lett. (2019), doi:http://dx.doi.org/10.1016/j.cclet.2019.12.014.
[22] G. Wang, J. Qin, X. Zhou, et al., Adv. Function. Mater. 28 (2018) 1806144.
[23] S. Li, L.X. Zhang, M.Y. Zhu, et al., Sens. Actuator. B -Chem. 249 (2017) 611–623.
[24] W. Tang, J. Wang, Sens. Actuator. B -Chem. 207 (2015) 66–73.
[25] H. Zhang, W. Shi, N. Gao, et al., Sens. Actuator. B -Chem. 296 (2019) 126633.
[26] X. Zhou, A. Wang, Y. Wang, et al., ACS Sens. 3 (11) (2018) 2385–2393.
[27] X. Zhou, Y. Zou, J. Ma, et al., Chem. Mater. 31 (2019) 8112–812.
[28] W. Shi, M.D.M. Ahmed, S. Li, et al., ACS Appl. Nano Mater. 2 (2019) 5430–5439.
[29] S. Ameen, M.S. Akhtar, H.S. Shin, Mater. Lett. 106 (2013) 254–258.
[30] J. Du, X. Huang, R. Zhao, J. Li, T. Asefa, Chem. Eur. J. 22 (2016) 8068–8073.
[31] Y. Yang, M. Li, Z. Zhu, Talanta 201 (2019) 295–300.
[32] X. Xin, Y. Zhang, X. Guan, et al., ACS Appl. Mater. Interfaces 11 (2019) 9438–9447.